Multifunctional Fully Textile Integrated RFID Tag to Revolutionise the Internet of Things in Clothing

Leticia Alonso-González, *Member, IEEE,* Samuel Ver-Hoeye, *Member, IEEE,* Carlos Vázquez-Antuña, Miguel Fernández-García, and Fernando Las-Heras Andrés, *Senior Member, IEEE*

***Abstract*—A novel multifunctional fully textile integrated radiofrequency identification tag has been designed, simulated and experimentally verified. The tag, which works at 13.56 MHz, is based on the inductive coupling phenomenon. It has been designed to be hidden from touch and sight, while being large-scale manufacturable. The manufactured prototype has been characterised and the theoretically predicted behaviour of the tag has been experimentally verified.**

***Index Terms*—Internet of things (IoT), radiofrequency identification (RFID), smart textile, textile antenna, wearables.**

I. Introduction

The ever growing interest in textile integrated devices has recently drawn attention to wearable identification, information storage and tracking systems, especially based on RFID technology. Due to the technological advances and decreased costs, the number of RFID based applications has dramatically increased, especially in the context of the Internet of Things (IoT). These applications have driven improvements in specific aspects of the technology, such as the range or working distance between reader and tag, or the data management capacity, which are closely linked to the operating frequency.

For instance, RFID technology is widely used nowadays in inventory tracking and item location, due to its advantages with regard to barcode technology, including unattended reading and increased range, among many others. RFID technology is regulated by different standardisation bodies, although the oldest established is ISO (International Standards Organisation). Several standards have been defined to regulate different aspects of RFID technology. As an example, ISO 18000-V3 defines the air interface for RFID systems working at 13.56 MHz. In addition, when working at 13.56 MHz, ISO 14443 defines the specifications for the use of RFID proximity cards for identity, security or payment applications, whereas ISO 15693 defines characteristics of the vicinity cards, which can be read from a larger distance than proximity cards. Vicinity cards are used in applications such as physical access, and therefore, they require a very short read range.

When working at a frequency of 13.56 MHz, as will be the case, an RFID antenna would be enormous. For this reason, low frequency RFID standards have not been developed to use antennas, but inductors. The operation is no longer based on the propagation of electromagnetic waves between the tag and the reader, but on an inductive coupling between them constituting a resonant circuit. For this reason, even though the frequency is very low, the read range is dramatically reduced and limited by the inductive coupling between the reader and the tag.

Several technologies have been used to develop both antenna and inductor based, RFID tags: from the ultra thin RFID tags embedded in paper, to the inkjet printed tags in plastic [1–4]. With the aim of integrating the RFID tags into the textile, some solutions have been presented. One of the proposed textile based RFID tags which can be found in the literature is based on an embroidery process [5–9], although these tags are not as industrially competitive as the conventional ones, due to the difficulty of manufacturing them in large scale production. Moreover, the embroidery process is not suitable for multilayered designs, and consequently, the number of possible design alternatives is reduced. For this reason, in the following sections, weaving technology is applied [11–15] for the development of a woven RFID tag. The proposed tag will be designed to be used in contactless applications, in particular, for stock identification during inventory, data storage and anti-imitation of clothing. Moreover, the prototype will be designed to be totally hidden from sight and touch, so that it can not be easily identified in the fabric.

The paper is organised as follows. In Section II, the structure of the tag will be presented. In Section III, the translation into a woven prototype will be explained. In Section IV, the tag will be simulated. The fabrication process will be presented in Section V. In Section VI, the experimental validation will be analysed.

II. Structure of the Tag

The tag is designed to operate according to ISO 15693, for its use at a frequency of 13.56 MHz. The communication at this frequency is realised through inductive coupling between the tag and the interrogator device, as has been previously mentioned. This means that the tag inductance has to be designed to resonate together with the tag chip at 13.56 MHz. For the present design, a NXP chip from the ICODE SLIX family has been chosen, presenting an input capacitance of C_S = 23.5 pF [10].

Fig. 1 depicts the ideal equivalent electrical parameters of the proposed tag. On the left hand side of the circuit, the inductive part of the tag, L_A, is presented. On the right hand side of the circuit, the capacitance C_S is included. The

Manuscript received October 7, 2017; revised March 13, 2017; accepted December 2, 2018. Date of publication February 26, 2015; date of current version April 02, 2015.

The authors are with the Signal Theory and Communications Area, Department of Electrical Engineering, University of Oviedo, Gijón E-33203, Spain (e-mail: alonsoleticia@uniovi.es).

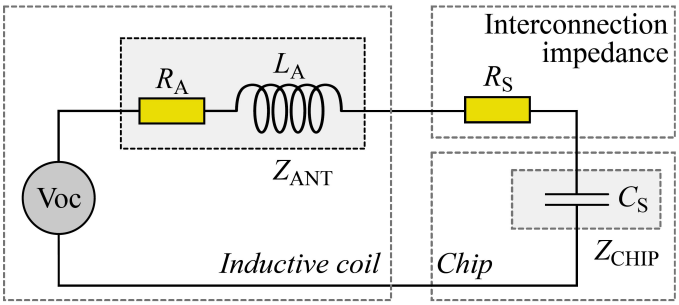

Fig. 1. Ideal equivalent electrical circuit of the proposed tag.

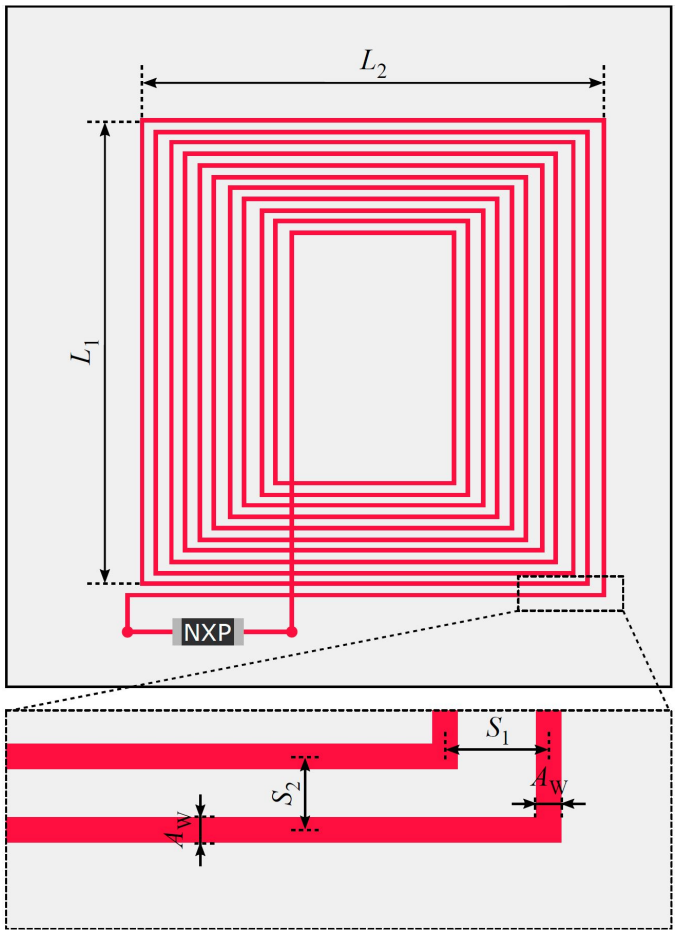

Fig. 2. Schematic drawing of the proposed RFID tag and magnification.

ohmic losses of the inductive coil and the interconnection impedance between the coil and the chip are given by R_A and R_S, respectively. The inductive part of the circuit can be achieved using a planar coil as the one depicted in Fig. 2.

The ideal equivalent circuit is modelled by a serial resonant circuit whose input impedance is given by the addition of the real and imaginary impedances previously defined. The resonant frequency is found at the frequency for which the imaginary part of the input impedance is equal to zero or, equivalently, the phase of the input impedance is equal to zero. At the working frequency, f_o, L_A and C_S must fulfil (1).

$$L_A C_S (2\pi f_o)^2 = 1 \tag{1}$$

Using the electromagnetic simulation software ADS, the equivalent electrical circuit of the proposed tag can be simulated, substituting the convetional inductor by a planar square loop coil model. This ADS library model is defined by the number of turns of the coil, the dimensions of the conductive material cross section, the distance between turns and the dimensions of the biggest turn, as well as the electrical conductivity.

An infinite number of combinations of these parameters can achieve the desired inductance, although not all of them can then be translated into a woven prototype. For this reason, the dimensions of the threads and the weaving loom limitations must be taken into account in the design.

III. Design of the Woven Prototype

For the conductive parts of the coil, *Shieldex 117f17 HC+B 1-ply* threads have been used. When these threads are in the woven structure, they present a Pierce's cross section. Consequently, this cross section is an ellipse whose horizontal and vertical axes are $A_W = 0.26$ mm and $A_H = 0.13$ mm, respectively. Therefore, the width of the conductive strips of the tag are approximated by A_W as depicted in Fig. 2.

With the aim of avoiding undesired short circuits, due to the existence of little yarns in the multifilament conductive threads, a sufficient separation between them must be adopted. Therefore, a distance of $S_1 = 2$ mm between the centres of the conductive threads in one of the directions, and a distance of $S_2 = 1.5$ mm in the perpendicular direction have been adopted.

When the before mentioned parameters S_1 and S_2 are different, there is not a predefined model in ADS to simulate the behaviour of the planar coil, therefore, Momentum has been employed for the design. By using 12 turns and being $L_1 = L_2 = 55$ mm, the external dimensions of the coil, the desired working frequency, $f_o = 13.56$ MHz, was achieved.

To translate the square loop of the tag into a textile prototype, a woven structure composed of three layers has been designed. The top layer is composed of dielectric warp and weft threads, except in certain positions where the warp threads have been substituted by conductive *Shieldex* yarns. These positions correspond to twenty-three warp threads divided in two groups of 11 and 12 threads, respectively. The bottom layer is composed of dielectric warp and weft threads, except in certain positions where the weft threads have been substituted by conductive *Shieldex* yarns. These positions correspond to twenty-two weft threads divided in two groups of 11 threads each. The before mentioned top and bottom layers are independent and electrically isolated from each other by an additional dielectric layer which is woven between them, giving rise to a total thickness of the woven structure of $T_S = 0.35$ mm.

The conductive warp and weft yarns in the top and bottom layers must be interconnected at specific locations, in order to configure the desired coil-shaped current path, as shown in Fig. 3. The interconnections are realised by bringing the

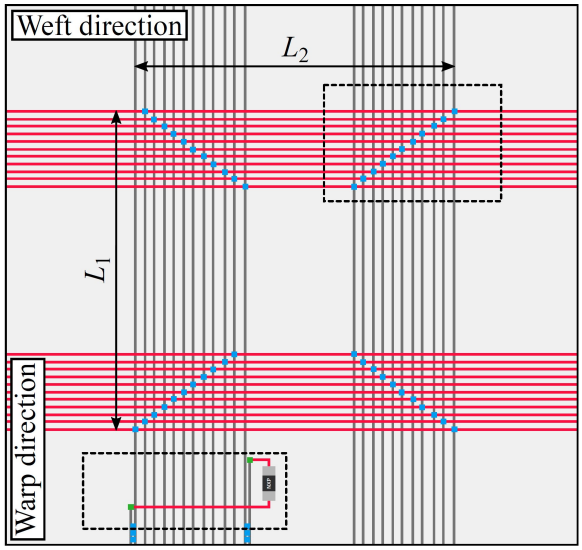

(a)

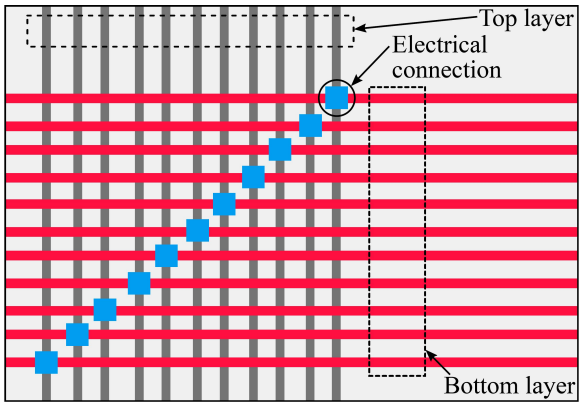

(b)

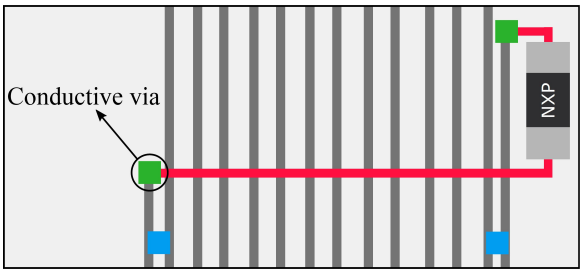

(c)

Fig. 3. Overview of the RFID tag design and magnifications (bottom view). (a) General view of the tag. (b) Magnification of the electrical connections. (c) Magnification of the chip interconnection.

desired conductive weft yarn from the bottom layer vertically up, across the intermediate dielectric layer, weaving it around the corresponding warp yarn in the top layer, and taking it back to the bottom layer to continue its normal weaving pattern. This direct contact between conductive threads produces the required electrical connection.

Fig. 3a depicts the bottom view of the RFID tag, where the dielectric threads have not been represented for simplification. Nevertheless, conventional multifilament polyester threads have been employed for the dielectric parts of the design. For the warp and weft threads, 0.07 mm and 0.35 mm

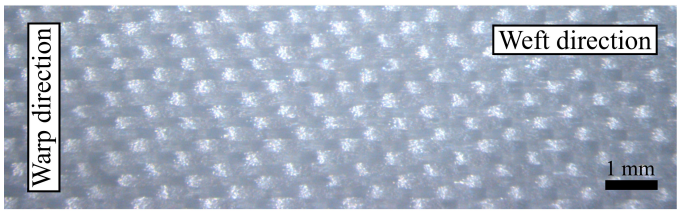

Fig. 4. Overview of the woven substrate.

diameter yarns have been employed, leading to the substrate depicted in Fig. 4. The substrate has been characterised using an Agilent Technologies 85072A Split Cylinder Resonator and its relative dielectric permittivity and loss tangent have been found to be $\varepsilon_{subs} = 1.5$ and $\tan(\delta)_{subs} = 0.0025$, respectively.

Conductive warp threads corresponding to the top layer are grey colored, whereas the conductive weft threads which correspond to the bottom layer are red colored. The electrical connection between the conductive threads and the connection of the chip are blue and green colored, respectively. Fig. 3b depicts a magnification where the layers to which each conductive thread belongs is indicated. Fig. 3c represents a magnification of the chip interconnection.

IV. Simulations

The ideal equivalent electrical parameters of the tag have been simulated using ADS, without taking into account the possible existence of parasitic capacitive effects in the coil. Consequently, the circuit depicted in Fig. 1 has been simulated. With the aim of achieving a resonant frequency of 13.56 MHz, L_A has been found to be 5.86 μH.

By measuring the lengths of all the conductive threads required to conform the coil in the Momentum model, and multiplying the total length by the resistance of the *Shieldex* thread, 3 Ω/cm, then R_A has been found to be 440 Ω. The interconnection impedance is given by the conductive paths between the terminals of the coil and the terminals of the chip. A total length of three centimetres has been estimated for these conductive paths, then the interconnection impedance, R_S, has been found to be 9 Ω.

The ideal equivalent electrical model has been simulated and Fig. 5 depicts the imaginary part and the phase of the input impedance, Z_{IN}. A zero crossing has been achieved in 13.56 MHz.

V. Fabrication Process

Once the textile coil has been designed, the woven prototype can be manufactured following two steps. First, the textile coil needs to be woven and secondly, the chip must be integrated in the woven structure. The textile coil has been manufactured using an industrial MüGrip loom.

Once the textile planar inductor is manufactured, the NXP chip needs to be integrated in the woven coil. Fig. 6 depicts the dimensions of the chip and its contacts, $W_{CHIP} = 0.47$ mm, $W_T = 1.09$ mm and $L_T = 2.84$ mm. Due to the fact that the distance between the woven coil terminals is larger than the distance between the contacts of the chip, an adapting path is

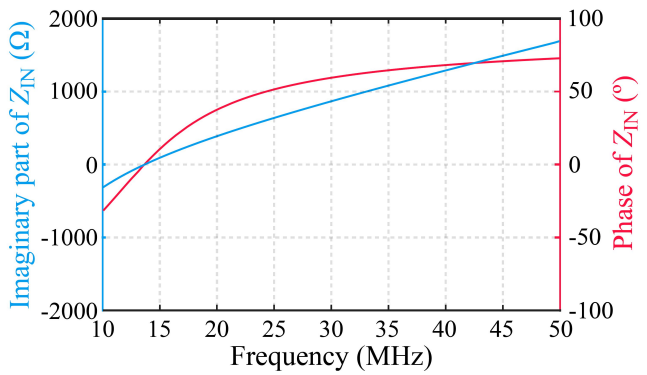

Fig. 5. Simulated imaginary part and phase of the input impedance of the tag using the ideal equicalent model.

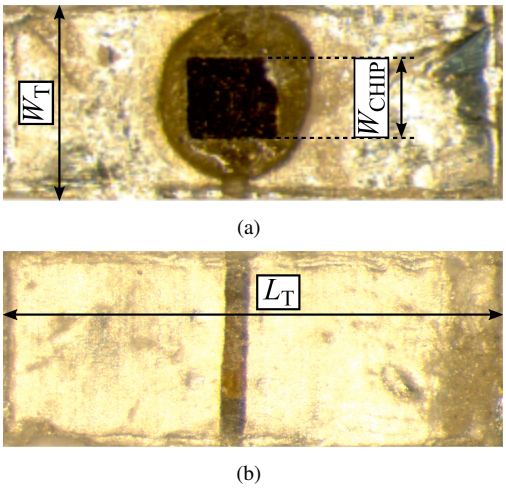

Fig. 6. Overview of the chip and dimensions. (a) Top view. (b) Bottom view.

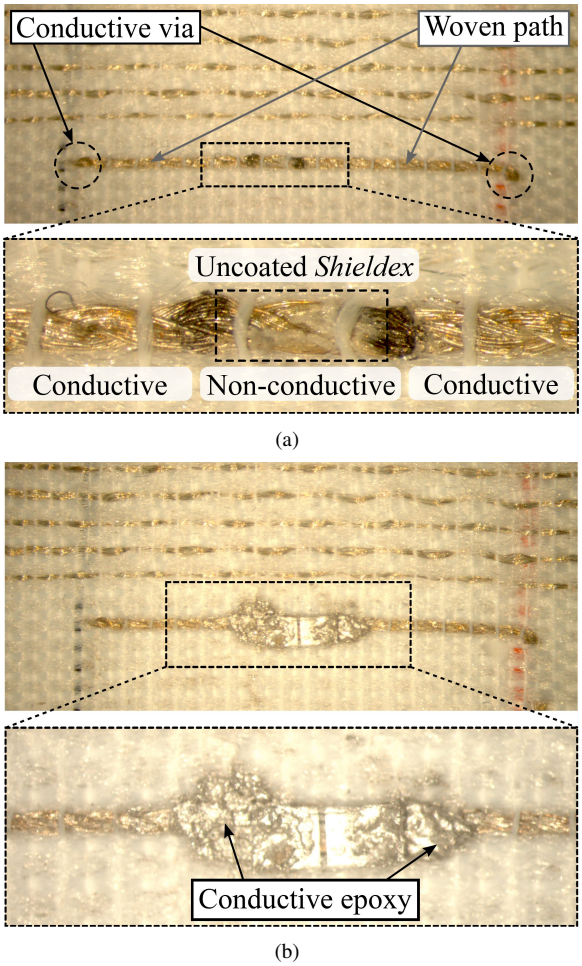

Fig. 7. Process of the chip integration by treating the Shieldex thread and using epoxy glue. (a) Conductive vias and magnification of the woven path. The uncoated *Shieldex* section is not conductive and corresponds to the chip footprint. (b) Integrated chip and magnification of the epoxy connections.

required. To achieve this path, short circuiting the conductive threads between the terminals of the coil has to be avoided.

With the aim of integrating the chip in the woven coil while avoiding the undesired short circuits, several alternatives have been analysed. Isolating the conductive warp threads from the adapting path by the use of a dielectric paste has been discarded, since the textile would acquire a different texture. This would not be interesting when trying to hide the tag. Therefore, with the aim of solving this problem, two different alternatives, based on electrically conductive vias, are presented, with the novelty of connecting the chip in the bottom layer of the tag.

The first proposed method to integrate the NXP chip in the tag is based on using a single *Shieldex* thread which has been uncoated at the place where the chip will be mounted and corresponding to the footprint of the chip. This thread is a new warp thread which is electrically connected to both terminals of the woven coil in the top layer. The *Shieldex* thread crosses the prototype, from the top to the bottom layer, by using conductive vias as depicted in Fig. 7a. In the bottom layer, the *Shieldex* thread is isolated from the other conductive warp threads, then it is able to cross the layer. In the area where the *Shieldex* thread has been uncoated, the chip can be connected by the use of conductive epoxy adhesive as depicted in Fig. 7b.

The second proposed alternative to integrate the chip in the tag is based on the use of two silver warp monofilaments. Each silver monofilament is electrically connected to each terminal of the coil as in the first method, an both silver monofilaments cross the prototype from the top layer to the bottom layer through conductive vias. Consequently, each silver monofilament can then be welded to each pad of the chip.

The second proposed alternative to integrate the chip has been found to be the most advisable option, due to the fact that the welding process is easier to automate than the uncoating process. Consequently, the second proposed method has been employed during the experimental validation. The resultant textile prototype is depicted in Fig. 8 and Fig. 9. Fig. 8 represents the top view of the manufactured prototype and a magnification where the dimensions of the conductive threads are detailed. Fig. 9 depicts the bottom view of the manufactured prototype and a magnification where the chip is integrated by the use of silver monofilaments.

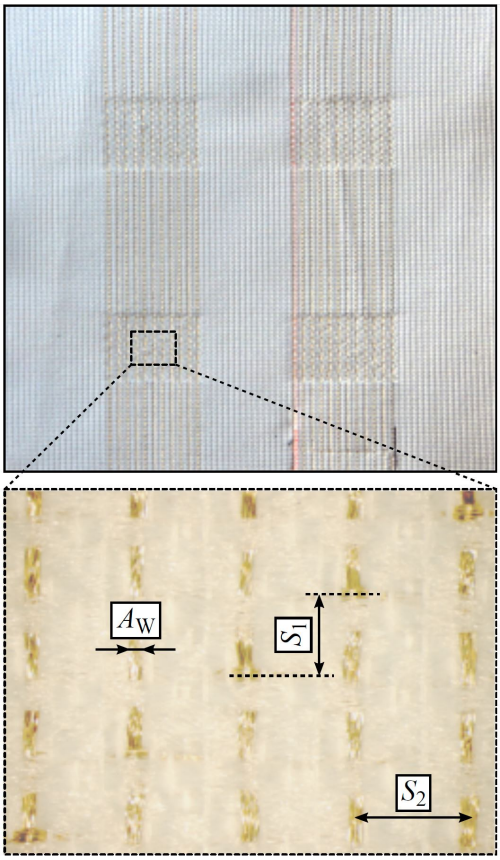

Fig. 8. Top view of the manufactured prototype using the silver warp monofilament for the chip integration and detailed magnification of the dimensions.

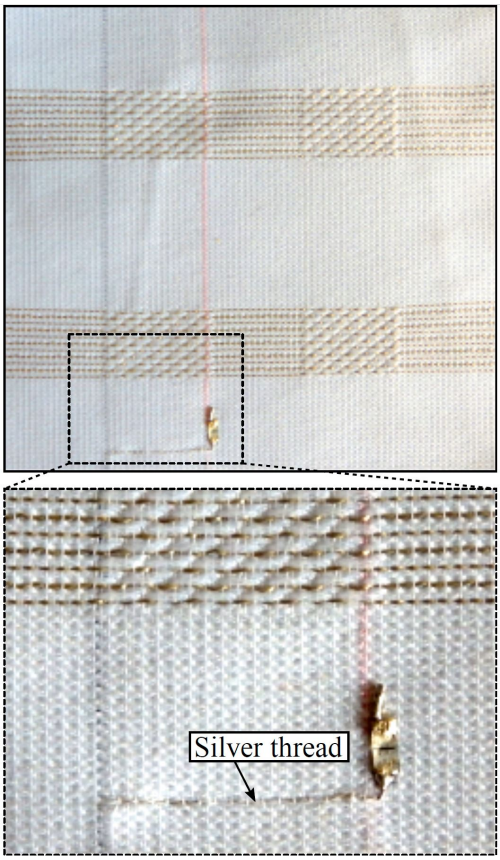

Fig. 9. Bottom view of the manufactured prototype and detailed magnification of the silver warp monofilament for the chip integration.

VI. Experimental validation

The experimental validation of the prototype has been carried out using a PNA-X N5247A vector network analyser from Agilent Technologies. For the DC experimental characterisation, a Keysight Technologies U1252B multimeter has been used.

In order to have a more accurate model of the manufactured prototytpe, the experimental interconnection impedance $R_{S'}$ has been measured and found to be $11.1\ \Omega$. The input impedance of the coil in DC, $R_{A'}$, without taking into account the interconnection has also been measured and found to be $444\ \Omega$. Due to the existence of parasitic capacitive effects in the textile coil, the self resonance of the tag could be measured and was found to be 19.4 MHz, as depicted in Figure 10a (solid line).

Using the aforementioned experimental values and the frequency response of the self resonance, a more accurate ADS model has been achieved by adjusting the parameters shown in Fig. 11. The impedance $R_{A'}$ has been divided into two impedances, $R_{A'1}$ and $R_{A'2}$, which have been found to be $160\ \Omega$ and $284\ \Omega$, respectively. The new resonant componentes, $C_{A'}$ and $L_{A'}$, have been adjusted and found to be 9 pF and 5.5 μH, respectively. Another impedance, R_C, in series with the parasitic capacitor has been required and found to be $35\ \Omega$.

Fig. 10a represents a comparison between the frequency response of the self resonance using the new simulated model and corresponding measurements. Fig. 10b depicts the complete frequency response of the woven tag. A good agreement between the simulations and the results has been achieved.

After characterising the frequency response of the textile tag, the prototype has been tested using a smartphone as interrogator. As it could be anticipated taking into account the resistive loss of the conductive threads, the read range of the inductive RFID tag is a few centimetres, which are sufficient for the proposed applications.

Moreover, the tag has also been tested under different conditions. First, the tag has been bent in order to verify the performance of the electrical connections. As the electrical connections are achieved by the contact between conductive threads, then the tag continues working properly after the bending test. Furthermore, the tag has also been tested after five washing processes, obtaining a positive result.

VII. Conclusion

A fully textile based tag for its use in clothing has been discussed. It presents several advantages in comparison with existing conventional RFID tags, including its potential for large scale production in the context of textile manufacturing, or the possibility of integrating the tag in clothing, hiding it from sight and touch.

Furthermore, the material around the coil can be mostly reduced. Consequently, the amount of conductive material to manufacture the proposed tag is comparable to its analogous

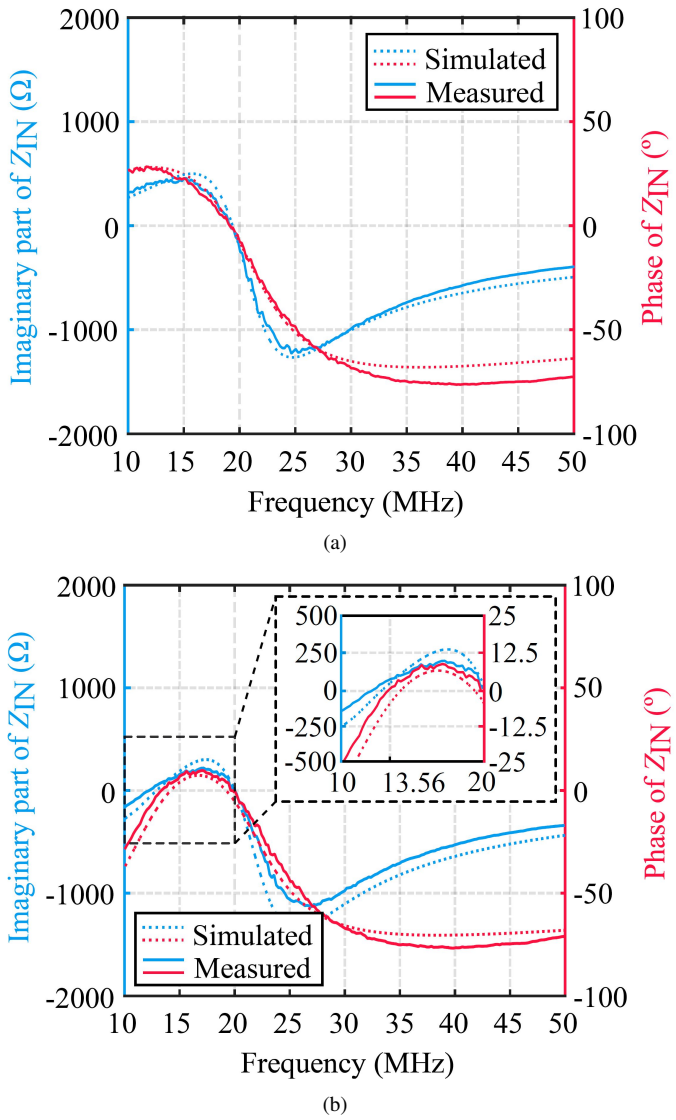

Fig. 10. Imaginary part and phase of the input impedance of the tag. (a) Simulated self resonance (dotted lines). Measured self resonance (solid lines). (b) Equivalent electrical model of the tag in Figure 11, and magnification. Simulated response (dotted lines). Measured response (solid lines).

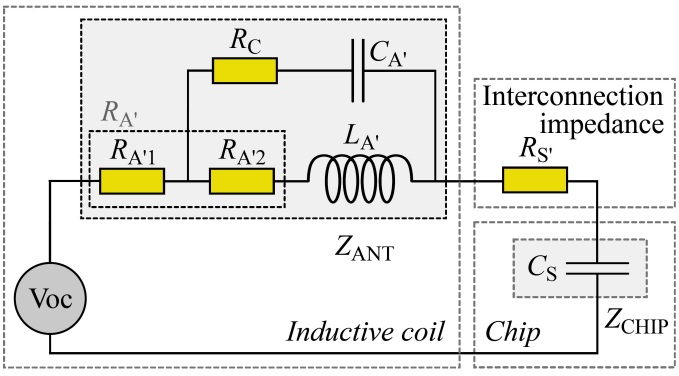

Fig. 11. Equivalent electrical circuit of the proposed tag taking into account the self resonance.

using embroidery procedures. However, weaving technology allows a level of large scale production which cannot be achieved with embroidery alternatives.

Thanks to the RFID chip, information regarding the product in which this tag has been located can be stored, not only for inventory or authentication, but also for customer information. This data could include information currently available in different uncomfortable labels attached to the clothing, or even purchase date details, avoiding the use of sales receipts. The introduction of RFID technology in clothing has an endless number of interesting applications which are the future of the textile industry.

In this paper, different alternatives for the design of the tag and the integration of the chip have been discussed and a final prototype has been proposed. The translation into a woven structure has been explained in detail, as well as the characteristics of the employed materials. An equivalent circuit of the proposed prototype has been presented and electromagnetic simulations and experimental results have been compared. A good agreement between simulations and experimental results has been achieved.

ACKNOWLEDGMENT

This work has been supported by the Spanish Agencia Estatal de Investigación (AEI) and Fondo Europeo de Desarrollo Regional (FEDER) under projects TEC2016-80815-P (AEI/FEDER-UE) and TEC2015-72110-EXP (AEI), and FPU14/00016 grant, and by the Gobierno del Principado de Asturias (PCTI/FEDER-FSE) under projects IDI/2016/000372 and IDI/2017/000083.

REFERENCES

[1] V. Lakafosis *et al.*, "Progress towards the first wireless sensor networks consisting on inkjet-printed, paper-based RFID-enabled sensor tags", *Proc. IEEE*, vol. 98, no. 9, pp. 1601-1609, Sep. 2010.

[2] S. Dey and N. C. Karmakar, "Design and analysis of a novel low cost high data capacity chipless RFID tag on plastic substrate", presented in *46th European Microw. Conf.*, London, UK, Sep. 2016.

[3] M. Akbari *et al.*, "Implementation and performance evaluation of graphene-based passive UHF RFID textile tags", presented in *Int. Symp. Electromagnetic Theory*, Espoo, Finland, Aug. 14-18, 2016.

[4] W. G. Whittow *et al.*, "Inkjet-printed microstrip patch antennas realized on textile for wearable applications", *IEEE Antennas Wireless Propag. Lett.*, vol. 13, pp. 71-74, 2014.

[5] G. Ginestet *et al.*, "Embroidered antenna-microchip interconnections and contour antennas in passive UHF RFID textile tags", *IEEE Antennas Wireless Propag. Lett.*, vol. 16, pp. 1205-1208, 2017.

[6] A. Paraskevopoulos *et al.*, "Higher-mode textile patch antenna with embroidered vias for on-body communication", *IET Microw. Antennas and Propag.*, vol. 10, no. 7, pp. 802-807, May 2016.

[7] A. Kiourti, C. Lee and J. L. Volakis, "Fabrication of textile antennas and circuits with 0.1 mm precision", *IEEE Antennas Wireless Propag. Lett.*, vol. 15, pp. 151-153, May 2016.
[8] Z. Wang *et al.*, "Embroidered conductive fibers on polymer composite for conformal antennas", *IEEE Trans. Antennas Propag.*, no. 9, pp. 4141-4147, Sep. 2012.
[9] T. Acti *et al.*, "Embroidered wire dipole antennas using novel copper yarns", *IEEE Antennas Wireless Propag. Lett.*, vol. 14, pp. 638-641, Nov. 2015.
[10] NXP Icode Slix Product family datasheet, HF-RFID. [Online]. Available: https://www.nxp.com/docs/en/brochure/75016918.pdf
[11] L. Alonso-González *et al.*, "Fully textile-integrated microstrip-fed slot antenna for dedicated short-range communications" in *IEEE Trans. Antennas and Propag.*, vol. 66, no. 5, pp. 2262-2270, May 2018.
[12] L. Alonso-González *et al.*, "Three-Dimensional Fully Interlaced Woven Microstrip-Fed Substrate Integrated Waveguide," in *Progress In Electromagnetics Research*, Vol. 163, 25-38, 2018.
[13] L. Alonso-González *et al.*, "Layer-to-Layer Angle Interlock 3D Woven Bandstop Frequency Selective Surface," in *Progress In Electromagnetics Research*, Vol. 162, 81-94, 2018.
[14] L. Alonso-Gonzlez *et al.*, "Broadband flexible fully textile-integrated bandstop frequency selective surface," in *IEEE Trans. Antennas and Propag.*, vol. 66, no. 10, pp. 5291-5299, Oct. 2018.
[15] L. Alonso-González *et al.*, "On the techniques to develop millimeter-wave textile integrated waveguides using rigid warp threads" in *IEEE Trans. Microw. Theory and Techniques*, vol. 66, no. 2, pp. 751-761, Feb. 2018.
[16] M. Mantash *et al.*, "Design methodology for wearable antenna on artificial magnetic conductor using stretch conductive fabric," *Electron. Lett.*, vol. 52, no. 2, pp. 95-96, 2016.
[17] NXP Icode Slix Product family datasheet, HF-RFID. [Online]. Available: http://www.nxp.com/documents/leaflet/75016918.pdf

Leticia Alonso-González (alonsoleticia@uniovi.es) received her Ph.D. degree in electrical engineering from the University of Oviedo (Spain) in 2018. She is currently a Research Fellow specialised in the development of fully textile-integrated microwave circuits and antennas with the Signal Theory and Communications Group, University of Oviedo.

Samuel Ver-Hoeye (versamuel@uniovi.es) received his Ph.D. degree in electrical engineering from the University of Cantabria (Spain) in 2002. He is currently an Associate Professor with the Department of Electrical Engineering, University of Oviedo (Spain). His main research interests are focused on the design and analysis of nonlinear oscillator based circuits, millimetre-wave/THz antennas, circuits and systems, graphene based components and textile-integrated circuits and antennas.

Carlos Vázquez-Antuña (vazquezcarlos@uniovi.es) received his Ph.D. degree in electrical engineering from the University of Oviedo (Spain) in 2013. He is currently a Research Fellow specialised in nonlinear analysis and optimisation techniques for the design of oscillator-based circuits with the Signal Theory and Communications Group, University of Oviedo.

Miguel Fernández-García (fernandezgmiguel@uniovi.es) received his Ph.D. degree in electrical engineering from the University of Oviedo (Spain) in 2010. He is currently an Associate Professor with the Signal Theory and Communications Group, University of Oviedo. His main research interests include nonlinear analysis and optimisation techniques for the design of multifunctional oscillator-based circuits, active antennas and passive components.

Fernando Las-Heras Andrés (flasheras@uniovi.es) received his Ph.D. degree in electrical engineering from the Technical University of Madrid (Spain) in 1990. He is currently a Full Professor and the head of the Signal Theory and Communications Group, University of Oviedo. He is a Senior Member of the IEEE and a member of the IEEE Microwaves and Antennas Propagation Chapter (AP03/MTT17) Board from 2016 to 2018.